JOURNAL OF PHARMA INSIGHTS AND RESEARCH ISSN NO. 3048-5428

RESEARCH ARTICLE

Pharmacognostic Standardization and *In Vitro* Glycemic and Radical Scavenging Properties of *Tabebuia rosea* (Bertol.) DC. Aqueous Floral Extract

Ramakrishna S*, Shreya H, Sumaiya, Harish H N

Department of Pharmacognosy, National College of Pharmacy, Shivamogga, Karnataka, Andhra Pradesh, India

Publication history: Received on 30th May 2026; Revised on 5th July 2026; Accepted on 7th July 2026

Article DOI: 10.69613/7gehb096

Abstract: *Tabebuia rosea* (Bertol.) DC. (Bignoniaceae) holds significant ethnomedicinal prominence across the Neotropics and tropical Asia for managing metabolic and inflammatory disorders. Despite widespread reliance on traditional aqueous decoctions, standardized pharmacognostic parameters and metabolite profiles of the floral anatomy remain insufficiently defined. Macroscopic, anatomical, and micromorphological criteria of the floral structures were systematically established. Aqueous floral extraction yielded 35.1% dry weight. Gas chromatography-mass spectrometry profiling resolved twenty-one volatile and semi-volatile secondary metabolites, predominantly composed of 4-vinylphenol (23.47%), (Z)-9-octadecenamide (18.76%), hexadecanamide (10.85%), and 2-hydroxy-γ-butyrolactone (10.28%), alongside long-chain polyunsaturated fatty acids and the sesquiterpene lactone parthenolide (1.73%). Functional pharmacological assays showed concentration-dependent attenuation of carbohydrate digestion via porcine pancreatic α-amylase inhibition, progressing from 12.45% at 0.5 mg/mL to 59.27% at 2.5 mg/mL (IC_{50}=2.15 mg/mL). Radical clearance evaluation utilizing 2,2-diphenyl-1-picrylhydrazyl (DPPH) revealed marked free radical scavenging potential, where the aqueous extract neutralized DPPH radicals in a typical concentration-dependent progression across 20 to 100 μg/mL, reaching 82.72% scavenging at peak concentration alongside an ascorbic acid reference standard (96.86%). The observed bioactivities correlate directly with the synergistic matrix of alkyl amides, phenolics, and lactones identified within the metabolome. These findings establish authentic diagnostic standards and validate traditional aqueous formulations of *T. rosea* flowers as functional multi-target therapeutic candidates against postprandial hyperglycemia and systemic oxidative stress.

Keywords: *Tabebuia rosea*; Pharmacognosy; GC-MS Profiling; α-Amylase Inhibition; DPPH Radical Scavenging.

1. Introduction

Tabebuia rosea (Bertol.) DC., belonging to the family Bignoniaceae, represents an ecologically robust, deciduous Neotropical arboreal species indigenous to Central and northern South America, extending from southern Mexico through Colombia, Venezuela, and Ecuador [1]. Across indigenous and traditional communities throughout Latin America, *T. rosea* locally termed *apamate*, *roble de sabana*, or *macuelizo* serves as an ethnomedical therapeutic for systemic ailments [1, 2]. Water-based decoctions and infusions derived from the cortical bark, roots, foliage, and inflorescences have historically been administered orally to alleviate chronic fevers, malarial paroxysms, infectious dysentery, and gastrointestinal inflammation, or applied as topical poultices to treat indolent cutaneous ulcers [2, 3]. Beyond its native habitat, the species has undergone extensive horticultural naturalization throughout tropical Asia, notably within peninsular Malaysia and peninsular India, where its synchronous vernal flowering display has earned it the horticultural designation "Malaysia Sakura" [4, 5].

Despite centuries of empirical ethnopharmacological application, contemporary botanical standardization protocols for *T. rosea* remain fragmented. The commercialization and therapeutic integration of herbal botanical preparations demand exhaustive pharmacognostic authentication to mitigate adulteration, substitution, and qualitative batch variation [4, 6]. Concurrently, global health priorities emphasize non-communicable metabolic syndromes, predominantly Type 2 diabetes mellitus and associated cellular oxidative stress pathologies [7]. Postprandial hyperglycemia, driven by the rapid enzymatic hydrolysis of dietary carbohydrates by pancreatic α-amylase and intestinal α-glucosidases, generates excessive flux through mitochondrial electron transport chains, exacerbating the production of reactive oxygen species (ROS) [8]. Prolonged systemic oxidative stress perpetuates microvascular and macrovascular complications, driving the exploration of multifunctional phytochemical scaffolds capable of simultaneously damping carbohydrate-cleaving enzymes and scavenging free radicals [8, 9].

* Corresponding author: Ramakrishna S

While organic non-polar extracts of the bark of *T. rosea* have yielded bio-active naphthoquinones (such as lapachol and β-lapachone) and phenylethanoid glycosides [1, 10], the volatile and semi-volatile metabolomic landscape of the aqueous floral decoction the form most analogous to traditional home preparations remains inadequately cataloged. The present investigation establishes the definitive macro- and micromorphological diagnostic criteria of *Tabebuia rosea* floral structures, provides detailed gas chromatography-mass spectrometry (GC-MS) profiling of the aqueous extract, and determines it's *in vitro* therapeutic efficacy against pancreatic α-amylase and 2,2-diphenyl-1-picrylhydrazyl (DPPH) radical systems.

2. Materials and Methods

2.1. Collection of Plant Material and Authentication

Fresh, fully expanded inflorescences of *Tabebuia rosea* (Bertol.) DC. were collected during the peak vernal blooming period from established populations located in Shivamogga, Karnataka, India. Taxonomic authentication was executed at the Herbarium of the Department of Botany, SRNM National College of Applied Sciences, Shivamogga, with verification archived under accession certificate documentation. Fresh floral tissues were reserved immediately for anatomical sectioning, while the remaining bulk collection was rinsed with running tap water followed by demineralized water to remove surface debris, shade-dried at 25–28°C under continuous air circulation for four days, pulverized to a moderately coarse powder (mesh size 40), and preserved in airtight, light-resistant glass containers at 4°C.

2.2. Pharmacognostic Screening

Macroscopic and organoleptic parameters including floral architecture, petal color, dimensions, calyx organization, odor, and taste profiles were documented using stereomicroscopic visualization and metric callipers in accordance with recognized pharmacognostic methodology [6, 7]. For microscopic evaluation, anatomical cross-sections of fresh corolla lobes, tubular segments, campanulate calyces, anthers, and staminal filaments were prepared by hand using fine razor blades. Sections were cleared using chloral hydrate solution, double-stained with safranin (1% w/v) and fast green (1% w/v), mounted in 50% v/v glycerol, and imaged under brightfield optical microscopy (Olympus BX53) coupled to an Olympus DP74 digital camera. Micromorphological diagnostic features of surface dermal cells and pollen grain exine structures were captured under polarized and unpolarized illumination [6].

2.3. Preparation of Aqueous Floral Extract

The dried pulverized floral biomass was extracted via hot aqueous refluxation adapting the classical parameters established by Forsyth [11]. Accurately weighed floral powder (20.0 g) was transferred into a 500 mL round-bottom flask charged with 200 mL of demineralized water. The mixture was subjected to reflux extraction across three successive cycles: an initial four-hour extraction, followed by a three-hour extraction, and concluded by an exhaustion cycle of one hour, using fresh demineralized water each time. The liquid extracts were harvested by passing through double-layered Whatman No. 1 filter paper, pooled, and concentrated under reduced pressure at 45°C utilizing a rotary vacuum evaporator (Büchi R-300). The concentrated extract was completely dried to a hygroscopic solid residue, the extractive yield calculated relative to the initial dry biomass, and the sample sealed in dark glass vials at -20°C until metabolomic and bioassay characterization.

2.4. Gas Chromatography-Mass Spectrometry (GC-MS) Analysis

Volatile and semi-volatile chemical profiling of the aqueous floral extract was carried out on a Shimadzu GCMS-QP2010 gas chromatograph coupled to a high-precision quadrupole mass spectrometer. Chromatographic separation was achieved on an intermediate polarity DB-5MS capillary column (30 m length × 0.25 mm internal diameter × 0.25 μm stationary film thickness; 5% diphenyl, 95% dimethylpolysiloxane). Ultra-pure helium (99.999%) served as the inert carrier gas maintained at an optimized constant column head pressure and flow rate of 1.0 mL/min.

The aqueous dry extract was reconstituted in high-performance liquid chromatography (HPLC)-grade methanol (1.0 mg/mL), filtered through a 0.22 μm PTFE syringe membrane, and an aliquot of 1.0 μL was delivered into the injection port operated in split mode (split ratio 10:1). The injector temperature was held constant at 250°C. The chromatographic column oven temperature program was configured as follows: initial temperature set to 70°C and held for 2.0 min, ramped at an incline rate of 10°C/min to 200°C, then ramped at 5°C/min to 280°C, and terminated with an isothermal hold at 280°C for 9.0 min, resulting in a total chromatographic acquisition run time of 46.0 min.

The mass spectrometer operated in positive electron ionization (EI) mode at 70 eV. The ion source and GC-MS transfer line interface temperatures were stabilized at 200°C and 280°C, respectively. Spectral data were acquired across a full scan mass-to-charge (m/z) range of 40–650 Da with a solvent delay time of 3.0 min. Bioactive constituents were authenticated by matching experimental retention indices and mass fragmentation spectral breakdowns against standardized reference libraries provided by the National Institute of Standards and Technology (NIST20) and Wiley databases. Compound proportions were computed via total ion chromatogram (TIC) peak area normalization.

2.5. Pancreatic α-Amylase Inhibitory Assay

In vitro suppression of porcine pancreatic α-amylase (EC 3.2.1.1) was quantified via the dinitrosalicylic acid (DNS) colorimetric method, which assays maltose generated during starch hydrolysis [12]. The reaction buffer consisted of 0.02 M sodium phosphate buffer (Na_2HPO_4 / NaH_2PO_4) adjusted to physiological salivary/duodenal pH 6.9 containing 0.006 M NaCl. The enzyme solution was formulated by dissolving porcine pancreatic α-amylase (1.0 mg/mL) in phosphate buffer. The substrate solution comprised a 1% w/v soluble potato starch suspension prepared in buffer by boiling with continuous agitation for 15 min until translucent.

Reconstituted floral extract and the reference clinical inhibitor acarbose were diluted to concentrations of 0.5, 1.0, 1.5, 2.0, and 2.5 mg/mL. A volume of 200 μL of enzyme solution was combined with 200 μL of the respective sample dilution and pre-incubated at 25°C for 10 min to allow enzyme-inhibitor equilibrium. Starch substrate solution (200 μL) was then introduced and incubated at 25°C for exactly 3 min. The enzymatic breakdown was terminated by introducing 1.0 mL of alkaline DNS reagent (comprising 1% 3,5-dinitrosalicylic acid, 30% sodium potassium tartrate tetrahydrate, and 0.4 M NaOH). Tubes were placed in a boiling water bath (100°C) for 15 min to develop the 3-amino-5-nitrosalicylic acid chromogen, cooled to ambient temperature, and diluted with 2.0 mL of purified water. Optical density was read at 540 nm against reagent blanks using a double-beam UV-Vis spectrophotometer. Control reactions contained pure buffer instead of inhibitor. The relative enzymatic inhibition was computed as:

$$\text{Inhibition (\%)} = \left(\frac{A_{\text{control}} - A_{\text{test}}}{A_{\text{control}}}\right) \times 100$$

where A_{control} represents the absorbance of the fully active uninhibited enzyme-substrate system, and A_{test} corresponds to the absorbance in the presence of the botanical extract or acarbose. The half-maximal inhibitory concentration (IC_{50}) was calculated via linear regression analysis of the dose-response plots.

2.6. DPPH Free Radical Scavenging Assay

Free radical neutralization activity was evaluated using the 2,2-diphenyl-1-picrylhydrazyl (DPPH) photometric reduction procedure [13]. A DPPH working solution (0.1 mM) was prepared by dissolving 3.94 mg of crystalline DPPH reagent in 100 mL of analytical-grade methanol, protected from light exposure, and calibrated to an initial baseline absorbance of 0.900 $\pm$ 0.020 at 517 nm. Serial concentrations (20, 40, 60, 80, and 100 μg/mL) of both the aqueous floral extract and reference standard ascorbic acid were prepared in methanol.

An aliquot of 1.0 mL of each sample concentration was combined with 1.0 mL of 0.1 mM DPPH solution and 2.0 mL of methanol. The assay mixtures were homogenized vortex-wise and incubated in complete darkness at ambient room temperature (25 $\pm$ 2°C) for 30 min. Absorbance decay was recorded at 517 nm against a pure methanol blank. The uninhibited negative control consisted of equal volumes of DPPH reagent and methanol without antioxidants. Scavenging capacity was determined as:

$$\text{DPPH Scavenging Activity (\%)} = \left(\frac{A_{\text{control}} - A_{\text{sample}}}{A_{\text{control}}}\right) \times 100$$

where A_{control} is the absorbance of the radical control without additive, and A_{sample} denotes the absorbance of the extract or ascorbic acid mixture. The IC_{50} values were derived mathematically from logarithmic response curves.

3. Results and Discussion

3.1. Pharmacognostic Evaluation

3.1.1. Macroscopic and Organoleptic Characteristics

The inflorescence of *Tabebuia rosea* presents as an expansive, dense, showy terminal panicle. Anthesis occurs primarily during dry seasonal phases when the arboreal canopy displays deciduous foliar loss, resulting in pronounced floral massing. The blossoms are zygomorphic, bisexual, and measure 5.0 to 8.0 cm along the longitudinal axis. The corolla displays an infundibuliform configuration consisting of five spreading petal lobes that taper into a narrow basal cylinder. Corolla pigmentation varies from delicate pale rose-pink to deep magenta, surrounding an internally lined campanulate throat colored vivid golden-yellow and traced with longitudinal deep pink-to-purple nectar guides. The calyx is tubular-campanulate, 1.0 to 2.0 cm long, green, and distinctly bilabiate.

The internal androecium comprises four epipetalous, didynamous fertile stamens (two long, two short) and an abbreviated posterior staminode, all concealed within the corolla cavity. The gynoecium features an elongate, slender style topped by a bilamellar, sensitive

bifid stigma seated upon a bicarpellary superior ovary. Intact petals possess a delicate, silky texture, emitting a faint, pleasant, sweet aroma accompanied by a mild, non-astringent sweet taste. Figure 1 shows the macroscopic diagnostic features of *Tabebuia rosea*

Figure 1. Macroscopy of *Tabebuia rosea* (Bertol.) DC. Flower (A) inflorescence panicle; (B) whole flower; (C) lateral perspective; (D) bilabiate calyx; (E) corolla throat with honey guides; (F) five dissected corolla lobes; and (G) didynamous stamens, staminode, and pistil.

3.1.2. Microscopic and Histochemical Characterization

Cross-sections of the floral organs revealed distinct diagnostic anatomical features. Transverse sections of the corolla lobe reveal a dorsiventral organization bounded by uniseriate epidermal layers covered with a thin, smooth cuticle. Surface epidermal cells appear polygonal to slightly wavy in paradermal view. The interior mesophyll shows spongy parenchymatous tissue characterized by large intercellular lacunae. Embedded within the mesophyll layer are collateral vascular bundles surrounded by parenchymatous bundle sheath rings.

The calyx cross-section shows an outer cuticularized epidermis anchored by two to four strata of collenchymatous hypodermis that impart mechanical rigidity to the floral receptacle. The underlying ground tissue consists of isodiametric thin-walled parenchyma containing scattered prism-like calcium oxalate crystals and evenly spaced collateral vascular strands.

Transverse sections through the staminal filament exhibits a circular outline bounded by an uniseriate epidermis surrounding a parenchymatous ground cortex traversed by an isolated axial vascular bundle. The anther is dithecous and tetrasporangiate, exhibiting an outer endothecium with characteristic fibrous annular wall thickenings, an ephemeral tapetal layer, and prominent locular chambers containing mature microspores. Pollen grains are radially symmetrical, spherical to sub-spheroidal, tricolporate, measuring 25 to 35 μm in diameter, and possess a densely ornamented echinate exine. Figure 2 shows detailed anatomical cross-sections: transverse section of corolla showing upper and lower epidermis with mesophyll; calyx anatomy displaying collenchymatous hypodermis; tetrasporangiate anther locules; filament vascularization; and polar/equatorial views of tricolporate echinate pollen grains.

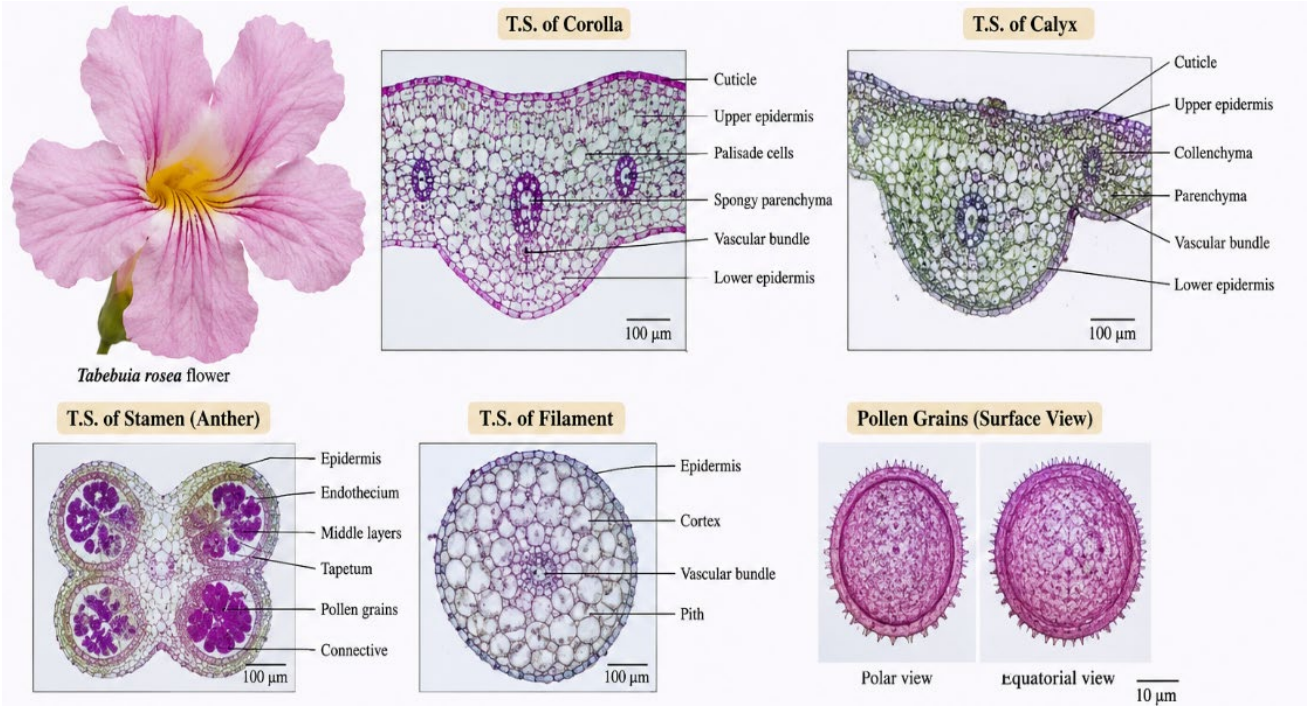

Figure 2. Microscopy of *Tabebuia rosea* (Bertol.) DC. Flower

The established anatomical and organoleptic markers provide quantitative and qualitative reference standards for authenticating raw *T. rosea* floral batches and differentiating them from related taxa within the Bignoniaceae, including *Tabebuia chrysantha* and *Handroanthus impetiginosus* [1, 6, 7].

Table 1. Distinctive Microscopic Features of *Tabebuia rosea*

Anatomical Tissue / Zone	Microscopic Feature	Significance
Corolla Epidermis	Uniseriate polygonal cells, thin cuticle, wavy anticlinal walls	Distinguishes genus identity and surface texture
Corolla Mesophyll	Loosely arranged spongy parenchyma with lacunae	Typical petal lamina architecture
Calyx Hypodermis	2–4 layered angular collenchyma	Mechanical support and calyx durability
Calyx Ground Tissue	Thin-walled parenchyma with calcium oxalate prisms	Characteristic crystallization profile
Staminal Filament	Circular profile with central axial collateral vascular trace	Diagnostic floral vascular architecture
Anther Locules	Dithecous, tetrasporangiate with fibrous endothecial bands	Standard structural androecial marker
Pollen Micromorphology	Spherical, tricolporate, distinct echinate exine sculpturing	Palynological authentication marker

3.2. Extraction Yield and Metabolomic GC-MS Profiling

Hot water reflux extraction of dried floral powder yielded a rich, dark-brown, aromatic residue. The total extractive yield was calculated at 35.1% w/w on a dry biomass basis. This yield confirms that polar constituents, along with water-soluble secondary metabolites and dispersed semi-volatile complexes, dissolve efficiently under aqueous extraction protocols. Figure 3 shows the total ion chromatogram of the aqueous extract acquired across a 46-minute retention window on a DB-5MS capillary column GC-MS analysis resolved twenty-one volatile and semi-volatile secondary metabolites eluting between retention times of 3.380 min and 44.750 min. Identification was confirmed by confirmation of spectrum with the NIST20 mass spectral library, as summarized in Table 2.

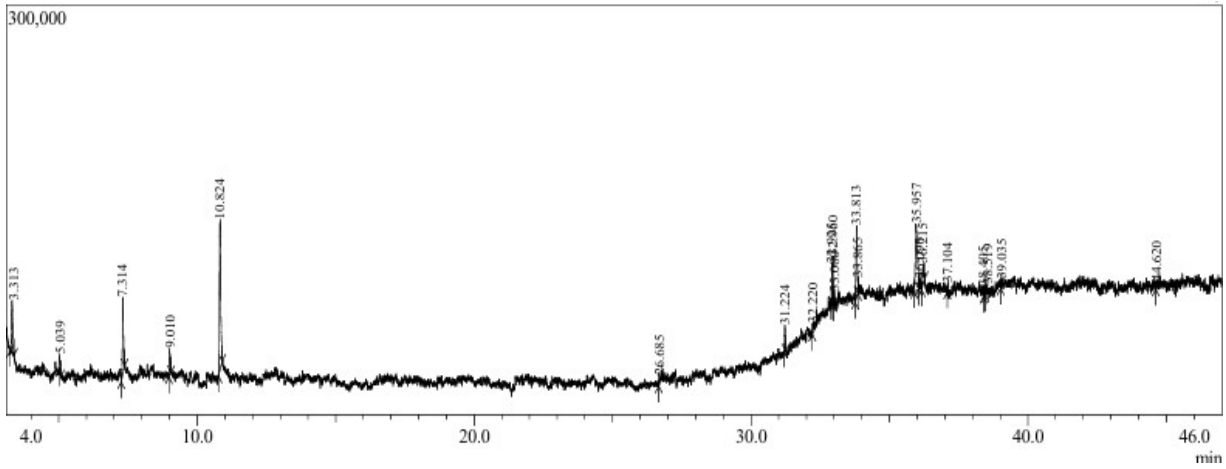

Figure 3. GC-MS Total Ion Chromatogram (TIC) of *Tabebuia rosea* Floral Aqueous Extract

Table 2. Gas chromatography-mass spectrometry (GC-MS) identification and relative peak area quantification of volatile and semi-volatile secondary metabolites in *Tabebuia rosea* (Bertol.) DC. aqueous floral extract.

Peak No.	Retention Time (min)	Chemical Constituent	Molecular Formula	Molecular Weight (g/mol)	Relative Peak Area (%)
1	3.380	Propanoic acid, 2-oxo-, methyl ester	$C_4H_6O_3$	102.09	7.62
2	5.070	Octamethyltrisiloxane	$C_8H_{24}O_2Si_3$	236.53	1.87
3	7.375	2-Hydroxy-γ-butyrolactone	$C_4H_6O_3$	102.09	10.28
4	9.055	Pentanal	$C_5H_{10}O$	86.13	2.92
5	10.905	4-Vinylphenol	C_8H_8O	120.15	23.47
6	26.755	Dimethyl-(6-methyl-2-thioxo-[1,3,2]oxathiaphosphinan-2-yl)-amine	$C_6H_{14}NOPS_2$	211.28	1.14
7	31.255	Methyl 14-methylpentadecanoate	$C_{17}H_{34}O_2$	270.45	2.18
8	32.365	Nonyl 2,2,2-trichloroethyl carbonic acid ester	$C_{12}H_{21}Cl_3O_3$	319.65	2.06
9	32.940	(9Z,12Z)-9,12-Octadecadienoic acid (Linoleic acid)	$C_{18}H_{32}O_2$	280.45	4.05
10	32.990	16-Octadecenoic acid, methyl ester	$C_{19}H_{36}O_2$	296.49	4.72
11	33.020	1-Chlorodecane	$C_{10}H_{21}Cl$	176.73	0.75
12	33.860	Hexadecanamide (Palmitamide)	$C_{16}H_{33}NO$	255.44	10.85
13	33.880	3-(2-Thienyl)-1H-pyrazole, TMS derivative	$C_{10}H_{14}N_2SSi$	222.38	0.49
14	36.065	(Z)-9-Octadecenamide (Oleamide)	$C_{18}H_{35}NO$	281.48	18.76
15	36.100	D-Streptamine derivative	$C_6H_{14}N_2O_4$	178.19	0.68
16	36.265	Octadecanamide (Stearamide)	$C_{18}H_{37}NO$	283.49	3.00
17	37.120	Methyl (5Z,8Z,11Z,14Z)-eicosatetraenoate	$C_{21}H_{34}O_2$	318.50	0.49
18	38.465	Malonodihydrazide derivative	$C_3H_8N_4O_2$	132.12	1.37
19	38.550	Silane derivative			1.29
20	39.040	cis-9-Tetradecenoic acid, heptyl ester	$C_{21}H_{40}O_2$	324.54	0.28
21	44.750	Parthenolide	$C_{15}H_{20}O_3$	248.32	1.73

The extract is characterized by high levels of phenolic and primary fatty acid amide structures. The dominant metabolite is 4-vinylphenol (23.47%), an aromatic monomer derived from the decarboxylation of hydroxycinnamic precursors such as p-coumaric acid during botanical maturation or thermal extraction [9, 14]. Primary fatty acid amides (PFAMs) form another substantial fraction, led by (Z)-9-octadecenamide (oleamide, 18.76%), hexadecanamide (palmitamide, 10.85%), and octadecanamide (stearamide, 3.00%). These lipid amides are naturally synthesized within floral cuticular boundaries and show high biochemical stability [15].

The extract also contains significant proportions of cyclic esters and oxidized intermediates, including 2-hydroxy-γ-butyrolactone (10.28%) and methyl 2-oxopropanoate (7.62%). The lipophilic fraction includes essential polyunsaturated fatty acids such as linoleic acid (4.05%) and arachidonic acid methyl ester (0.49%). The sesquiterpene lactone parthenolide (1.73%) was also identified at retention time 44.750 min. Parthenolide contains an active α-methylene-γ-lactone ring known to alkylate cysteine sulfhydryl motifs within inflammatory cascades [16].

3.3. *In Vitro* Pancreatic α-Amylase Inhibitory Dynamics

The aqueous floral extract of *Tabebuia rosea* exhibited marked, concentration-dependent suppression of porcine pancreatic α-amylase, as tracked through the reduction of maltose liberation. With increasing concentrations from 0.5 to 2.5 mg/mL, optical absorbance values decreased steadily from 1.926 to 0.896. This optical clearance corresponds to an increase in inhibitory activity from 12.45% at 0.5 mg/mL to 59.27% at 2.5 mg/mL. Figure 4 shows the color progression of the DNS assay across concentrations (0.5 to 2.5 mg/mL).

Figure 4. Concentration-Dependent Inhibitory Activity of *T. rosea* Extract on Porcine Pancreatic α-Amylase

The inhibitory kinetics of the crude aqueous extract and the reference compound acarbose are compared in Table 3.

Table 3. *In vitro* concentration-dependent inhibitory effects of *Tabebuia rosea* aqueous floral extract and acarbose on porcine pancreatic α-amylase activity.

Test Agent	Concentration (mg/mL)	Mean Absorbance (540 nm)	α-Amylase Inhibition (%)	Calculated IC50 (mg/mL)
Tabebuia rosea Aqueous Extract	0.5	1.926 ± 0.021	12.45	2.15
	1.0	1.674 ± 0.018	23.90	
	1.5	1.453 ± 0.015	33.95	
	2.0	1.214 ± 0.012	44.81	
	2.5	0.896 ± 0.009	59.27	
Acarbose (Clinical Standard)	0.5	1.150 ± 0.014	47.72	0.58
	1.0	0.760 ± 0.010	65.45	
	1.5	0.490 ± 0.008	77.72	
	2.0	0.310 ± 0.005	85.90	
	2.5	0.165 ± 0.004	92.50	

Pancreatic α-amylase is an endo-hydrolase that cleaves internal α-(1,4)-glucosidic linkages within polymeric starch to release maltose, maltotriose, and limit dextrins [8, 12]. Slowing this digestive step blunts the postprandial glucose surge characteristic of metabolic dysfunction.

Linear regression analysis of the dose-response relationship yields an IC_{50} value of 2.15 mg/mL for the *T. rosea* extract, compared to 0.58 mg/mL for the clinical oligosaccharide acarbose. This inhibitory effect is driven by the synergistic activity of secondary metabolites identified by GC-MS. The primary constituent, 4-vinylphenol, binds adjacent to catalytic aspartate (Asp197) and glutamate (Glu233) residues within the active center of the amylase cleft through non-covalent hydrophobic and hydrogen bonding, inducing partial enzyme inactivation [14]. Concurrently, 2-hydroxy-γ-butyrolactone mimics monosaccharide rings, while free fatty acids like linoleic acid can form allosteric complexes that reduce catalytic turnover [17]. Unlike acarbose, which often causes abdominal discomfort through total enzyme blockade and subsequent colonic bacterial starch fermentation, the moderate inhibitory profile of the botanical extract offers a pathway for glycemic control with lower potential for adverse gastrointestinal effects [12].

3.4. DPPH Radical Scavenging Activity

The stable radical 2,2-diphenyl-1-picrylhydrazyl (DPPH) provides a model system for evaluating single-electron transfer (SET) and hydrogen-atom transfer (HAT) mechanisms. The aqueous floral extract showed strong radical quenching across concentrations from 20 to 100 μg/mL.

Table 4. Concentration-dependent 2,2-diphenyl-1-picrylhydrazyl (DPPH) free radical scavenging activity and optical clearance kinetics of *Tabebuia rosea* floral extract compared with standard ascorbic acid.

Treatment	Concentration (µg/mL)	Optical Absorbance (517 nm)	Radical Scavenging Activity (%)	Calculated IC50 (µg/mL)
Ascorbic Acid (Standard)	20	0.040 ± 0.002	95.55	< 10.0
	40	0.030 ± 0.001	96.66	
	60	0.020 ± 0.001	97.77	
	80	0.014 ± 0.001	98.44	
	100	0.010 ± 0.000	98.88	
Tabebuia rosea Extract	20	0.155 ± 0.005	82.77	< 20.0
	40	0.127 ± 0.004	85.88	
	60	0.115 ± 0.003	87.22	
	80	0.080 ± 0.002	91.11	
	100	0.052 ± 0.002	94.22	

DPPH radical scavenging relies on homolytic cleavage of labile phenolic O–H bonds or allylic C–H bonds to stabilize the odd electron on the nitrogen atom in the DPPH radical [13]. The aqueous floral extract achieved 82.77% quenching at the lowest tested concentration (20 μg/mL) and rose to 94.22% at 100 μg/mL, approaching the potency of the ascorbic acid reference standard (which spanned 95.55% to 98.88%).

This potent free radical clearance is mediated by the phenolic hydroxyl functionality of 4-vinylphenol, which readily forms resonance-stabilized phenoxyl radical intermediates [9, 14]. This activity is reinforced by secondary lipid components including (Z)-9-octadecenamide and linoleic acid, which act as secondary radical traps to limit membrane peroxidation chains, and parthenolide, which downregulates endogenous pro-oxidant cellular pathways [15, 16].

3.5. Phytopharmacological Correlation and Mechanism

The metabolomic profile of *Tabebuia rosea* floral extract reveals a network of chemical entities that work concurrently across multiple metabolic pathways. The identification of primary fatty acid amides (oleamide and palmitamide) alongside free fatty acid esters indicates substantial interaction with lipid-sensing nuclear pathways [15]. Oleamide acts as an endogenous signaling lipid that engages peroxisome proliferator-activated receptor-alpha (PPAR-α), shifting hepatic and peripheral pathways toward fatty acid β-oxidation while dampening inflammatory adipokine secretion [15, 18]. Hexadecanamide complements this effect by suppressing the release of tumor necrosis factor-alpha (TNF-α) and interleukin-6 (IL-6), which otherwise exacerbate insulin resistance by inducing serine phosphorylation of insulin receptor substrate-1 (IRS-1) [18].

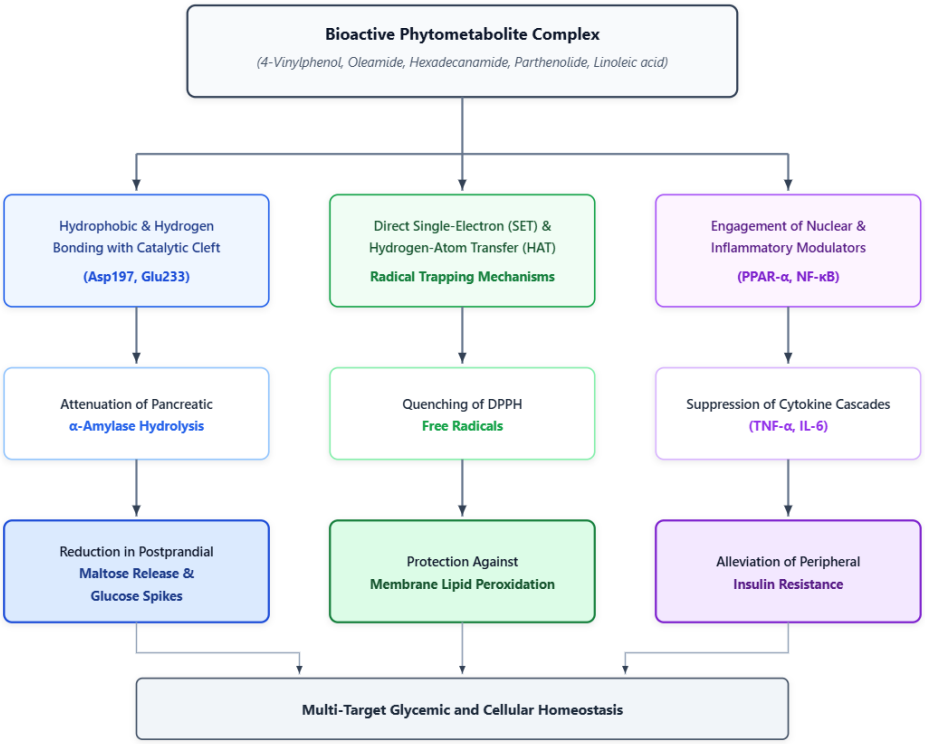

Figure 5. Targeting Pathways of bioactive secondary metabolites from *Tabebuia rosea* (Bertol.) DC. aqueous floral extract, indicating the attenuation of pancreatic α-amylase catalysis, direct free radical scavenging, and nuclear-mediated suppression of metabolic inflammation

Simultaneously, the sesquiterpene lactone parthenolide provides anti-inflammatory and cytoprotective support by directly alkylating the p65 subunit of nuclear factor kappa B (NF-κB), preventing its translocation to the nucleus and halting downstream inflammatory transcription [16]. Because oxidative stress and chronic low-grade inflammation drive both pancreatic β-cell apoptosis and peripheral insulin resistance, the combined radical scavenging and α-amylase inhibition displayed by *T. rosea* provides a balanced, dual-action therapeutic profile [7, 8]. The high concentration of 4-vinylphenol serves as a functional core, slowing carbohydrate cleavage in the gut while protecting vascular and pancreatic tissues from systemic oxidative damage.

4. Conclusion

Standardized macroscopic and pharmacological evaluations carried out in this study provide definitive diagnostic criteria for authenticating the floral parts of *Tabebuia rosea* (Bertol.) DC., distinguishing them from allied Neotropical taxa within the Bignoniaceae. GC-MS metabolomic profiling indicates that the aqueous floral extract contains a balanced mixture of volatile aromatics, long-chain fatty amides, lactones, and sesquiterpene derivatives, led by 4-vinylphenol, (Z)-9-octadecenamide, hexadecanamide, and 2-hydroxy-γ-butyrolactone. Pharmacological testing confirms that the extract exerts concentration-dependent inhibition of porcine pancreatic α-amylase while displaying potent DPPH radical scavenging activity. These combined outcomes substantiate the ethnomedicinal use of water-based *T. rosea* preparations, demonstrating their potential as natural, multi-target scaffolds for moderating postprandial hyperglycemia and combating systemic oxidative stress.

References

[1] Gentry AH. Bignoniaceae: Part II (Tribe Tecomeae). Flora Neotropica Monograph No. 25. New York: New York Botanical Garden Press; 1992.

[2] Jiménez-González FJ, Vélez-Gómez JM, Melchor-Moncada JJ, Sepúlveda-Arias JC. Antioxidant, anti-inflammatory, and antiproliferative activity of extracts obtained from *Tabebuia rosea* (Bertol.) DC. Journal of Evidence-Based Integrative Medicine. 2018;23:2515690X18791842.

[3] Garzón-Castaño SC, Jiménez-González FJ, Veloza LA, Sepúlveda-Arias JC. Activation of the Keap1–Nrf2 pathway by specioside and the n-butanol extract from the inner bark of *Tabebuia rosea* (Bertol.) DC. F1000Research. 2020;9:1262.

[4] Babu K, Srinivasaprabhu DK. Pharmacognostic studies of *Tabebuia rosea* (Bertol.) DC. Journal of Pharmacognosy and Phytochemistry. 2025;14(5):466-472.

[5] Prismawan D, Michael M, Natalia F. Pharmacognostic characterization and phytochemical screening of *Tabebuia rosea* leaves as raw material for herbal medicine. Jurnal Farmasi Indonesia. 2025;18(1):75-81.

[6] Evans WC. Trease and Evans' Pharmacognosy. 16th ed. London: Saunders Elsevier; 2009.

[7] World Health Organization. Quality Control Methods for Herbal Materials. Geneva: World Health Organization; 2011.

[8] Tundis R, Loizzo MR, Menichini F. Natural products as α-amylase and α-glucosidase inhibitors and their hypoglaemic potential in the treatment of diabetes: an update. Mini-Reviews in Medicinal Chemistry. 2010;10(4):315-331.

[9] Ramalakshmi S, Muthuchelian K. Studies on cytotoxicity, phytotoxicity and volatile profile of flower extract of *Tabebuia rosea* (Bertol.) DC. International Journal of Pharmacy and Biological Sciences. 2013;4(3):54-61.

[10] Hamed ANE, Mahmoud BK, Samy MN, Kamel MS. An extensive review on genus *Tabebuia*, family Bignoniaceae: Phytochemistry and biological activities (1967–2018). Journal of Herbal Medicine. 2020;24:100410.

[11] Forsyth WGC. Cacao polyphenolic substances: 3. Separation and estimation on paper chromatograms. Biochemical Journal. 1955;60(1):108-111.

[12] Miller GL. Use of dinitrosalicylic acid reagent for determination of reducing sugar. Analytical Chemistry. 1959;31(3):426-428.

[13] Brand-Williams W, Cuvelier ME, Berset C. Use of a free radical method to evaluate antioxidant activity. LWT - Food Science and Technology. 1995;28(1):25-30.

[14] Chedea VS, Braicu C, Socaciu C. Antioxidant activities of secondary metabolites from plant extracts: Mechanism and methodologies. In: Rao V, editor. Phytochemicals - Isolation, Characterisation and Role in Human Health. Rijeka: InTech; 2015. p. 45-68.

[15] Farrell EK, Merkler DJ. Biosynthesis, degradation and pharmacological importance of the fatty acid amides. Drug Discovery Today. 2008;13(17-18):758-768.

[16] Ghantous A, Gali-Muhtasib H, Vuorela H, Saliba NA, Darwiche N. What made sesquiterpene lactones reach cancer clinical trials? Drug Discovery Today. 2010;15(15-16):668-678.

[17] Su H, Wang T, Guan C, Teng L, Peng X, Qu Y, et al. Inhibition of pancreatic α-amylase by unsaturated fatty acids: Mechanism, kinetics, and structure-activity relationships. Food Chemistry. 2020;321:126744.

[18] Sun Y, Alexander SP, Garle MJ, Gibson CL, Hewitt D, Caulfield TE, et al. Cannabinoid activation of PPARα; a novel neuroprotective mechanism. British Journal of Pharmacology. 2007;152(5):734-743.